8

Cell Replication and Control

Michael C. Mackey, Caroline Haurie, and Jacques Bélair

8.1 Introduction

Though all blood cells are derived from hematopoietic stem cells, the regulation of this production system is only partially understood. Negative feedback control mediated by erythropoietin and thrombopoietin regulates erythrocyte and platelet production, respectively, and colony stimulating factor regulates leukocyte levels. The local regulatory mechanisms within the hematopoietic stem cells are also not well characterized at this point. Due to their dynamic character, cyclical neutropenia and other periodic hematological disorders offer a rare opportunity to more fully understand the nature of these regulatory processes. We review here the salient clinical and laboratory features of a number of periodic hematological disorders, and show through a detailed example (cyclical neutropenia) how mathematical modeling can be used to quantify and test hypotheses about the origin of these interesting and unusual dynamics. The emphasis is on the development and analysis of a physiologically realistic mathematical model including estimation of the relevant parameters from biological and clinical data, and numerical exploration of the model behavior and comparison with clinical data.

Hobart Reimann was an enthusiastic proponent of the concept of periodic diseases (Reimann 1963). None of these conditions has been as intensively studied as cyclical neutropenia, in which circulating neutrophil levels spontaneously oscillate from normal to virtually zero. This chapter reviews current knowledge about periodic hematological disorders, the hypotheses that have been put forward for their origin, and the analysis of these hypotheses through mathematical models. Some illustrative examples of these disorders are shown in Figure 8.1.

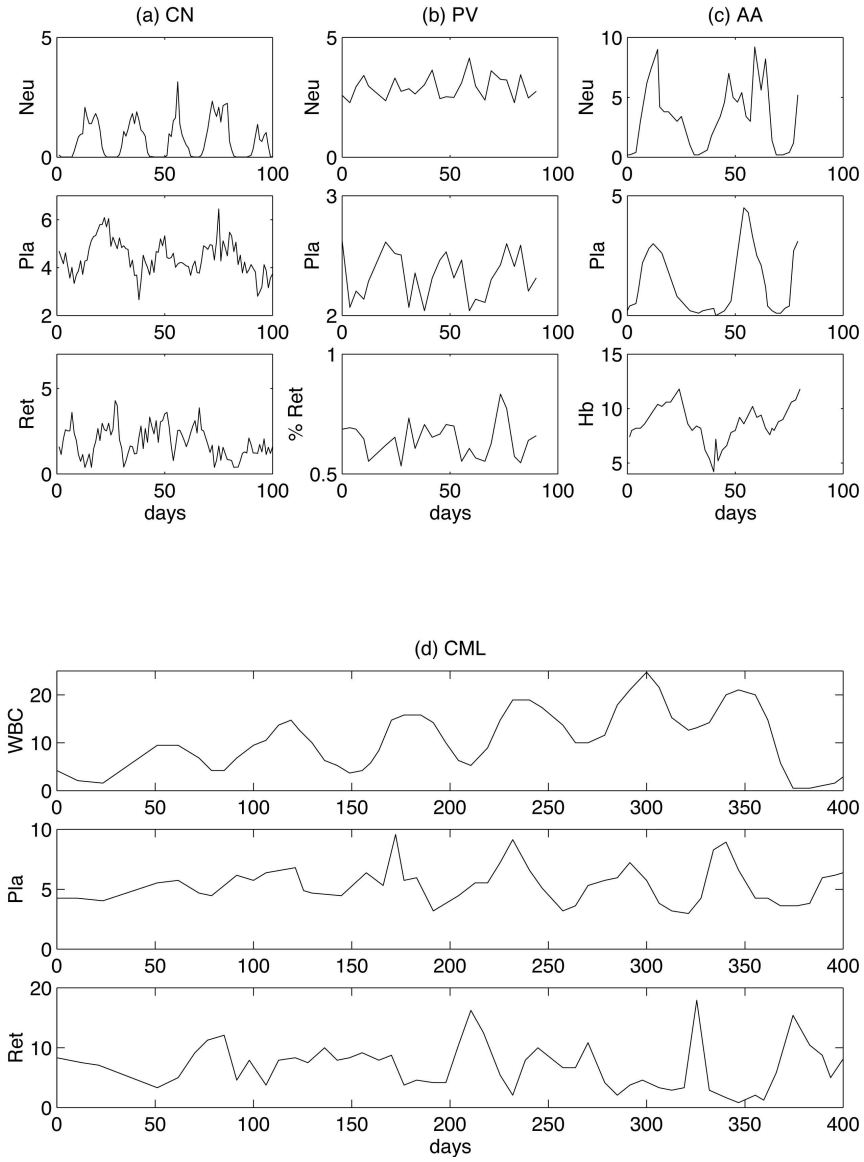

Figure 8.1. Representative patterns of circulating cell levels in four periodic hematological disorders considered in this chapter. Part (a) illustrates cyclical neutropenia (CN) (Guerry et al. 1973), (b) oscillations in polycythemia vera (PV) (Morley 1969), (c) oscillations in aplastic anemia (AA) (Morley 1979), and (d) periodic chronic myelogenous leukemia (CML) (Chikkappa et al. 1976). The density scales are: Neutrophils, 10^3 cells/mm^3; white blood cells, 10^4 cells/mm^3; platelets, 10^5 cells/mm^3; reticulocytes, 10^4 cells/mm^3; and Hb, g/dl. From Haurie, Mackey, and Dale (1998).

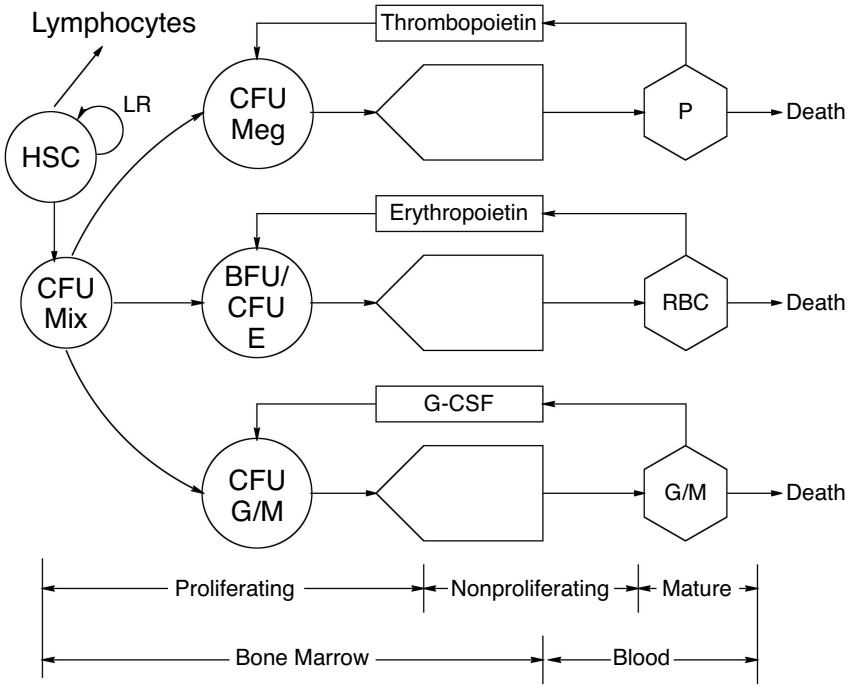

Figure 8.2. The architecture and control of hematopoiesis. This figure gives a schematic representation of the architecture and control of platelet (P), red blood cell (RBC), monocyte (M), and granulocyte (G) (including neutrophil, basophil, and eosinophil) production. Various presumptive control loops mediated by thrombopoietin, erythropoietin, and the granulocyte colony stimulating factor (G-CSF) are indicated, as well as a local regulatory (LR) loop within the totipotent hematopoietic stem cell population. CFU (BFU) refers to the various colony (burst) forming units (Meg = megakaryocyte, Mix = mixed, E = erythroid, and G/M = granulocyte/monocyte) which are the *in vitro* analogue of the *in vivo* committed stem cells. Adapted from Mackey (1996).

8.2 Regulation of Hematopoiesis

Although the regulation of blood cell production is complicated (Haurie et al. 1998), and its understanding constantly evolving, the broad outlines are clear.

Mature blood cells and recognizable precursors in the bone marrow ultimately derive from a small population of morphologically undifferentiated cells, the hemopoietic stem cells, which have a high proliferative potential and sustain hematopoiesis throughout life (Figure 8.2). The earliest hematopoietic stem cells are totipotent and have a high self-renewal capacity (Abramson et al. 1977; Becker et al. 1963; Lemischka et al. 1986), qualities that are progressively lost as the stem cells differentiate. Their

progeny, the progenitor cells, or colony forming units (CFU), are committed to one cell lineage. They proliferate and mature to form large colonies of erythrocytes, granulocytes, monocytes, or megakaryocytes. The growth of colony forming units *in vitro* depends on lineage-specific growth factors, such as erythropoietin,thrombopoietin, and the granulocyte, monocyte, and granulocyte/monocyte colony stimulating factors (G-CSF, M-CSF, and GM-CSF).

Erythropoietin adjusts erythropoiesis to the demand for O_2 in the body. A fall in tissue pO_2 levels leads to an increase in the renal production of erythropoietin. This in turn leads to an increased cellular production by the primitive erythroid precursors (CFU-E) and, ultimately, to an increase in the erythrocyte mass and hence the tissue pO_2 levels. This increased cellular production triggered by erythropoietin is due, at least in part, to an inhibition of programmed cell death (apoptosis) (Silva et al. 1996) in the CFU-E and their immediate progeny. Thus, erythropoietin mediates a negative feedback such that an increase (decrease) in the erythrocyte mass leads to a decrease (increase) in erythrocyte production. The regulation of thrombopoiesis involves similar negative feedback loops mediated by thrombopoietin.

The mechanisms regulating granulopoiesis are not as well understood. The granulocyte colony stimulating factor, G-CSF, the primary controlling agent of granulopoiesis, is known to be essential for the growth of the granulocytic progenitor cells CFU-G *in vitro* (Williams et al. 1990). The colony growth of CFU-G is a sigmoidally increasing function of the granulocyte colony stimulating factor, G-CSF (Avalos et al. 1994; Hammond et al. 1992). One of the modes of action of the granulocyte colony stimulating factor, along with several other cytokines, is to decrease apoptosis (Koury 1992; Park 1996; Williams et al. 1990; Williams and Smith 1993). Neutrophil maturation time also clearly shortens under the action of the granulocyte colony stimulating factor (Price et al. 1996). Several studies have shown an inverse relation between circulating neutrophil density and serum levels of granulocyte colony stimulating factor (Kearns et al. 1993; Mempel et al. 1991; Takatani et al. 1996; Watari et al. 1989). Coupled with the *in vivo* dependency of granulopoiesis on the granulocyte colony stimulating factor, this inverse relationship suggests that the neutrophils regulate their own production through a negative feedback, as is the case of erythrocytes: An increase (decrease) in the number of circulating neutrophils would induce a decrease (increase) in the production of neutrophils through the adjustment of the granulocyte colony stimulating factor levels. Although mature neutrophils bear receptors for the granulocyte (G-CSF) and for the granulocyte/monocyte (GM-CSF) colony stimulating factors, the role of these receptors in governing neutrophil production is not yet known.

Little is known about how the self-maintenance of the hematopoietic stem cell population is achieved, this self-maintenance of hematopoietic

stem cells depending on the balance between self-renewal and differentiation. Hematopoietic stem cells are usually in a dormant state but are triggered to proliferate after transplantation into irradiated hosts (Necas 1992), and the specific mechanisms regulating the differentiation commitment of hematopoietic stem cells are poorly understood (Ogawa 1993). However, mechanisms that could support autoregulatory feedback control loops controlling hematopoietic stem cell kinetics are starting to be investigated (Necas et al. 1988).

The selective responses of the erythrocytic, granulocytic, and megakaryocytic systems to increased demand of cell production indicate a relative autonomy of the peripheral control loops regulating these three cell lineages. The mechanisms regulating early hematopoiesis are, on the other hand, poorly understood, and strong connections may exist at this level between the regulation of the different blood lineages. In some of the periodic hematological disorders discussed here, such relations become visible though the occurrence of particular dynamical features common to all the blood lineages.

8.3 Periodic Hematological Disorders

We first introduce the main mathematical analysis technique we use to quantitatively assess the periodicity of clinical data.

8.3.1 Uncovering Oscillations

Fourier, or power spectrum, techniques are widely applicable when the data under study are evenly sampled but can give erroneous results when the data are unevenly sampled. While studying celestial phenomena, astrophysicists also encountered the problem of unevenly sampled data, and they developed an extension of the Fourier power spectrum, the Lomb periodogram, for evenly or unevenly sampled data (Lomb 1976). The statistical significance (p value) of any peak can also be determined (Scargle 1982). Thus the Lomb technique is ideally suited to the detection of periodicity in hematological time series, since serial blood counts are usually sampled at irregular intervals. Appendix C contains more details on the Lomb periodogram, $P(T)$, including its definition in equation (C.5).

8.3.2 Cyclical Neutropenia

General Features

Cyclical neutropenia has been the most extensively studied periodic hematological disorder. Its hallmark is a periodic fall in the circulating neutrophil

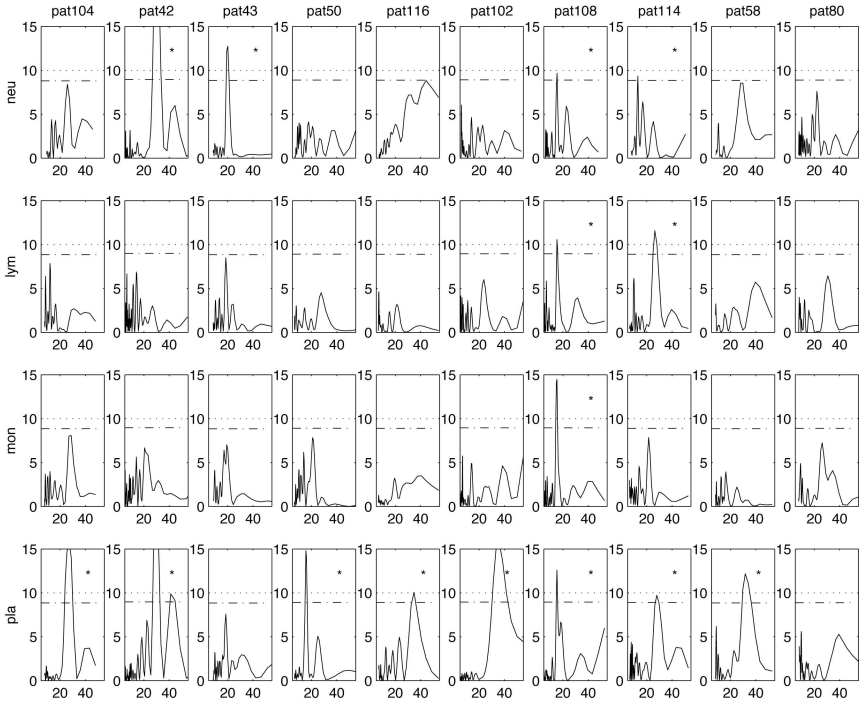

Figure 8.3. Lomb periodogram $P(T)$ [power P versus period T in days] of the blood cell counts of five cyclical neutropenia, three congenital neutropenic and two idiopathic neutropenic patients. The dotted lines in the Lomb periodogram give the $p = 0.10$ (lower dash–dot line) and $p = 0.05$ significance levels (upper dotted line); * indicates periodicity with significance $p \leq 0.10$. 'Neu': neutrophils, 'Lym': lymphocytes, 'Mon': monocytes, 'Pla': platelets. From Haurie, Mackey, and Dale (1999).

numbers from normal values to very low values. In humans it occurs sporadically or as an autosomal dominantly inherited disorder, and the period is typically reported to fall in the range of 19–21 days (Dale and Hammond 1988), though recent data indicate that the period may be as long as 46 days in some patients (Haurie et al. 1999) (see Figure 8.3).

Our understanding of cyclical neutropenia has been greatly aided by the discovery of an animal model, the grey collie (Figure 8.4). The canine disorder closely resembles human cyclical neutropenia with the exception of the period, which ranges from 11 to 15 days (Figure 8.5) (Haurie et al. 1999) and the maximum neutrophil counts, which are higher than for humans. For a review see Haurie, Mackey, and Dale (1998).

It is now clear that in both human cyclical neutropenia (Dale et al. 1972; Dale et al. 1972; Haurie et al. 1999; Hoffman et al. 1974) and the grey collie (Guerry et al. 1973; Haurie et al. 1999) there is not only a periodic

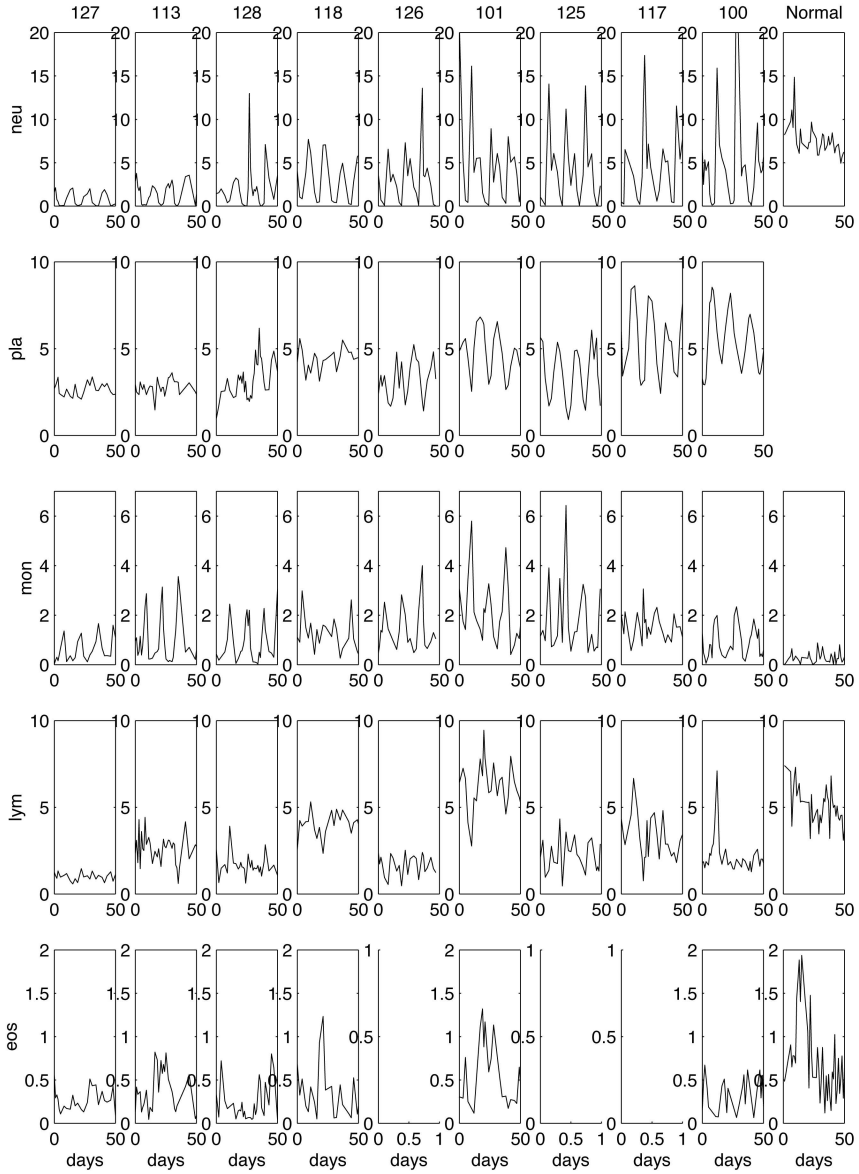

Figure 8.4. Differential blood counts in nine grey collies and one normal dog. Units: Cells $\times$ 10^{-5} per mm^3 for the platelets and Cells $\times$ 10^{-3} per mm^3 for the other cell types. 'Neu': neutrophils, 'Pla': platelets, 'Mon': monocytes, 'Lym': lymphocytes, 'Eos': eosinophils. From Haurie, Person, Mackey, and Dale (1999).

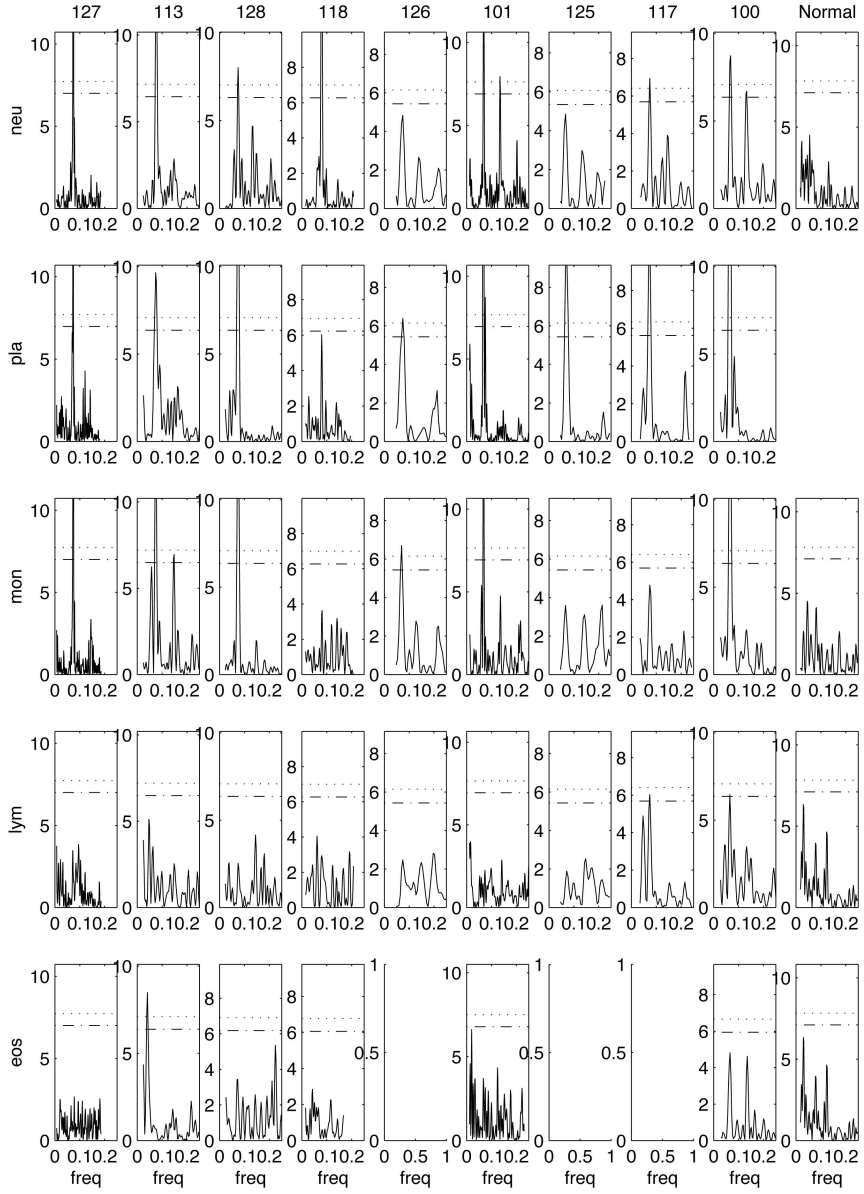

Figure 8.5. Lomb periodogram, equation (C.5), of the differential blood counts in nine grey collies. From Haurie, Person, Mackey, and Dale (1999).

fall in the circulating neutrophil levels, but also a corresponding oscillation of platelets, often the monocytes and eosinophils, and occasionally the reticulocytes and lymphocytes (see Figures 8.1A, 8.3, and 8.4). The mono-

cyte, eosinophil, platelet, and reticulocyte oscillations are generally from normal to high levels, in contrast to the neutrophils, which oscillate from near normal to extremely low levels. Often (but not always), the period of the oscillation in these other cell lines is the same as the period in the neutrophils.

The clinical criteria for a diagnosis of cyclical neutropenia have varied widely. Using periodogram analysis, some patients classified as having cyclical neutropenia do not, in fact, display any significant periodicity, while other patients classified with either congenital or idiopathic neutropenia do display significant cycling (Haurie et al. 1999) as shown in Figure 8.3. Moreover the period of the oscillations detected through periodogram analysis in neutropenic patients may be as long as 46 days (Haurie et al. 1999).

Origin

Transplantation studies show that the origin of the defect in cyclical neutropenia is resident in one of the stem cell populations of the bone marrow (Dale and Graw 1974; Jones et al. 1975; Jones et al. 1975; Weiden et al. 1974; Krance et al. 1982; Patt et al. 1973). Studies of bone marrow cellularity throughout a complete cycle in humans with cyclical neutropenia show that there is an orderly cell density wave that proceeds successively through the myeloblasts, promyelocytes, and myelocytes and then enters the maturation compartment before being manifested in the circulation (Brandt et al. 1975; Guerry et al. 1973). Further studies have shown that this wave extends back into the granulocytic progenitor cells (Jacobsen and Broxmeyer 1979) and erythrocytic progenitor cells (Dunn et al. 1977; Dunn et al. 1978; Hammond and Dale 1982; Jones and Jolly 1982), as well as in the erythrocytic burst forming units and granulocyte/monocyte colony forming units (Abkowitz et al. 1988; Hammond and Dale 1982), suggesting that it may originate in the totipotent hematopoietic stem cell populations.

Fluctuations in Putative Regulators

In cyclical neutropenia, the levels of colony stimulating activity (related to the granulocyte colony stimulating factor) fluctuate inversely with the circulating neutrophil levels and in phase with the peak in monocyte numbers (Dale et al. 1971; Guerry et al. 1974; Moore et al. 1974). Erythropoietin levels oscillate approximately in phase with the reticulocyte oscillation (Guerry et al. 1974). It is unclear whether these correlations and inverse correlations between levels of circulating cells and putative humoral regulators are related to the cause of cyclical neutropenia, or are simply a secondary manifestation of some other defect.

Effect of Phlebotomy and Hypertransfusion

The effect of bleeding and/or hypertransfusion on the hematological status of grey collies gives interesting results (Adamson et al. 1974). In the

untreated grey collie erythropoietin levels cycle out of phase with the reticulocytes and virtually in phase with the neutrophil counts. After phlebotomy (bleeding of between 10% and 20% of the blood volume), the cycles in the neutrophils and reticulocytes continue as before the procedure, and there is no change in the relative phase between the cycles of the two cell types. Hypertransfusion (with homologous red cells) completely eliminates the reticulocyte cycling (as long as the hematocrit remains elevated), but has no discernible effect on the neutrophil cycle. Most significantly, when the hematocrit falls back to normal levels and the reticulocyte cycle returns, the phase relation between the neutrophils and the reticulocytes is the same as before the hypertransfusion. These observations suggest that the source of the oscillations in cyclical neutropenia is relatively insensitive to any feedback regulators involved in peripheral neutrophil and erythrocyte control, whose levels would be modified with the alteration of the density of circulating cells; and is consistent with a relatively autonomous oscillation in the hematopoietic stem cells (cf. Section 8.5).

Effect of Cytokine Therapy

In both the grey collie (Hammond et al. 1990; Lothrop et al. 1988) and in humans with cyclical neutropenia (Hammond et al. 1989; Migliaccio et al. 1990; Wright et al. 1994) administration of the granulocyte colony stimulating factor leads to an increase in the mean value of the peripheral neutrophil counts by a factor of as much as 10 to 20, associated with a clear improvement of the clinical symptoms. However, the granulocyte colony stimulating factor does not obliterate the cycling in humans, but rather induces an increase in the amplitude of the oscillations and a decrease in the period of the oscillations in all the cell lineages, from 21 to 14 days (Hammond et al. 1989; Haurie et al. 1999).

8.3.3 Other Periodic Hematological Disorders Associated with Bone Marrow Defects

Periodic Chronic Myelogenous Leukemia

Chronic myelogenous leukemia is a hematopoietic stem cell disease characterized by granulocytosis and splenomegaly (Grignani 1985). In 90% of the cases, the hematopoietic cells contain a translocation between chromosomes 9 and 22, which leads to the shortening of chromosome 22, referred to as the Philadelphia (Ph) chromosome. In most cases, the disease eventually develops into acute leukemia.

In 1967, Morley was the first to describe oscillations in the leukocyte count of patients with chronic myelogenous leukemia (Morley et al. 1967). Several other cases of cyclic leukocytosis in chronic myelogenous leukemia have now been reported, and these have been reviewed in Fortin and Mackey (1999). In the cases of periodic chronic myelogenous leukemia, the

leukocyte count usually cycles with an amplitude of 30 to 200×10^9 cells/L and with periods ranging from approximately 30 to 100 days. The platelets and sometimes the reticulocytes also oscillate with the same period as the leukocytes, around normal or elevated numbers (Figure 8.1d). There have been no specific studies of hematopoiesis in patients with periodic chronic myelogenous leukemia.

Polycythemia Vera and Aplastic Anemia

Polycythemia vera is characterized by an increased and uncontrolled proliferation of all the hematopoietic progenitors, and it involves, like chronic myelogenous leukemia, the transformation of a single hematopoietic stem cell. Two patients with polycythemia vera were reported with cycling of the reticulocyte, platelet, and neutrophil counts in one case (Figure 8.1b), and cycling only of the reticulocyte count in the other. The period of the oscillations was 27 days in the platelets, 15 days in the neutrophils, and 17 days in the reticulocytes (Morley 1969).

Finally, clear oscillations in the platelet, reticulocyte, and neutrophil counts (Figure 8.1c) were reported in a patient diagnosed with aplastic anemia (Morley 1979) and in a patient with pancytopenia (Birgens and Karl 1993), with periods of 40 and 100 days, respectively.

Cytokine-Induced Cycling

The granulocyte colony stimulating factor, G-CSF, is routinely used in a variety of clinical settings, for example to treat chronic neutropenia or to accelerate recovery from bone marrow transplant and/or chemotherapy (Dale et al. 1993). The granulocyte colony stimulating factor may induce oscillations in the level of circulating neutrophils of neutropenic individuals (Haurie et al. 1999), and as will be seen later, in Section 8.5, this is of great significance in understanding cyclical neutropenia.

Induction of Cycling by Chemotherapy or Radiation

Several reports describe induction of a cyclical neutropenia-like condition by the chemotherapeutic agent cyclophosphamide. In mongrel dogs on cyclophosphamide the observed period was on the order of 11 to 17 days, depending on the dose of cyclophosphamide (Morley et al. 1969; Morley and Stohlman 1970). In a human undergoing cyclophosphamide treatment, cycling with a period of 5.7 days was reported (Dale et al. 1973). Also, Gidáli, István, and Fehér (1985) observed oscillations in the granulocyte and iculocyte counts with three weeks periodicity in mice after mild irradiation. They observed an overshooting regeneration in the reticulocytes and the thrombocytes but not in the granulocytes. While the CFU-S returned to normal levels rapidly, the proliferation rate of CFU-S stayed abnormally elevated.

Five patients with chronic myelogenous leukemia receiving hydroxyurea showed oscillations in their neutrophils, monocytes, platelets, and reticulocytes with periods in the range of 30 to 50 days (Kennedy 1970). In one patient an increase of the hydroxurea dose led to a cessation of the oscillations. Chikkappa et al. (1980) report a cyclical neutropenia-like condition (period between 15 and 25 days) in a patient with multiple myeloma after three years of chemotherapy.

A ^{89}Sr-induced cyclic erythropoiesis has been described in two congenitally anemic strains of mice, W/W^v and S1/S1^d (Gibson et al. 1984; Gibson et al. 1985; Gurney et al. 1981). W/W^v mice suffer from a defect in the hematopoietic stem cells, and in S1/S1^d mice the hematopoietic micro-environment is defective. The induction of cycling by ^{89}Sr can be understood as a response to elevated cell death (Milton and Mackey 1989), as can the dynamic effects of chemotherapy.

8.3.4 Periodic Hematological Disorders of Peripheral Origin

Periodic autoimmune hemolytic anemia is a rare form of hemolytic anemia in humans (Ranlov and Videbaek 1963). Periodic autoimmune hemolytic anemia, with a period of 16 to 17 days in hemoglobin and reticulocyte counts, has been induced in rabbits by using red blood cell autoantibodies (Orr et al. 1968).

Cyclic thrombocytopenia, in which platelet counts oscillate from normal to very low values, has been observed with periods between 20 and 40 days and reviewed in Swinburne and Mackey (2000). The cases in which there was an implication of an autoimmune source for the disease had periods between 13 and 27 days, while patients with the amegakaryocytic version have longer periods. From the modeling work of Santillan et al. (2000) it seems clear that the periodicity of the autoimmune version is probably induced through a supercritical Hopf bifurcation.

8.4 Peripheral Control of Neutrophil Production and Cyclical Neutropenia

8.4.1 Hypotheses for the Origin of Cyclical Neutropenia

Given the interesting dynamical presentation of cyclical neutropenia in both its clinical and laboratory manifestations, it is not surprising that there have been a number of attempts to model this disorder mathematically. In this section we briefly review these attempts, since they focus the work of this section and simultaneously motivate the extensions that we have made.

The mathematical models that have been put forward for the origin of cyclical neutropenia fall into two major categories. Reference to Figure 8.2 will help place these in perspective. (See Dunn 1983; Fisher 1993 for other reviews.)

The first group of models builds upon the existence of oscillations in many of the peripheral cellular elements (neutrophils, platelets, and erythroid precursors, see Figure 8.2) and postulates that the origin of cyclical neutropenia is in the common hematopoietic stem cell population feeding progeny into all of these differentiated cell lines. A loss of stability in the stem cell population is hypothesized to be independent of feedback from peripheral circulating cell types (see below) and would thus represent a relatively autonomous oscillation driving the three major lines of differentiated hematopoietic cells.

Mackey (1978) analyzed a model for the dynamics of a stem cell population and concluded that one way the dynamic characteristics of cyclical neutropenia could emerge from such a formulation was via an abnormally large cell death rate within the proliferating compartment. This hypothesis allowed the *quantitative* calculation of the period of the oscillation that would ensue when stability was lost. This hypothesis has been expanded elsewhere (Mackey 1979; Milton and Mackey 1989) and allows a qualitative understanding of the observed laboratory and clinical effects of the granulocyte colony stimulating factor and chemotherapy discussed above (Mackey 1996). In spite of the resonance of this stem cell origin hypothesis in the clinical and experimental communities (Quesenberry 1983; Ogawa 1993) there has been little extension of this hypothesis in the modeling literature related to cyclical neutropenia.

The second broad group of these models identifies the origin of cyclical neutropenia with a loss of stability in the peripheral control loop, operating as a sensor between the number of mature neutrophils and the control of the production rate of neutrophil precursors within the bone marrow (Figure 8.2). This control has been uniformly assumed to be of a negative feedback type, whereby an increase in the number of mature neutrophils leads to a decrease in the production rate of immature precursors. The other facet of this hypothesis is a significant delay due to the maturation times required between the signal to alter immature precursor production and the actual alteration of the mature population numbers. Typical examples of models of this type that have specifically considered cyclical neutropenia are Kazarinoff and van den Driessche (1979); King-Smith and Morley (1970); MacDonald (1978); Morley, King-Smith, and Stohlman (1969); Morley and Stohlman (1970); Morley (1979); Reeve (1973); von Schulthess and Mazer (1982); Shvitra, Laugalys, and Kolesov (1983); Schmitz (1988); Wichmann, Loeffler, and Schmitz (1988); Schmitz, Loeffler, Jones, Lange, and Wichmann (1990); Schmitz, Franke, Brusis, and Wichmann (1993); Schmitz, Franke, Loeffler, Wichmann, and Diehl (1994); Schmitz, Franke, Wichmann, and Diehl (1995); all of which have postulated an alteration

in the feedback on immature precursor production from the mature cell population numbers.

In the next section we show that it is highly unlikely that cyclical neutropenia is due to a loss of peripheral stability.

8.4.2 Cyclical Neutropenia Is Not Due to Peripheral Destabilization

Development. In the model development that follows, reference to the lower part of Figure 8.2, where the control of white blood cell production is outlined, will be helpful.

We let $x(t)$ be the density of white blood cells in the circulation (units of cells/μL blood), α be the random disappearance rate of circulating white blood cells (days^{-1}), and $\mathcal{M}_o$ be the production rate (cells/μL-day) of white blood cell precursors in the bone marrow.

The rate of change of the peripheral (circulating) white blood cell density is made up of a balance between the loss of white blood cells ($-\alpha x$) and their production ($\mathcal{M}_o(\tilde{x})$), or

$$\frac{dx}{dt} = -\alpha x + \mathcal{M}_o(\tilde{x}), \tag{8.1}$$

wherein $\tilde{x}(t)$ is $x(t-\tau)$ weighted by a distribution of maturation delays, $\tilde{x}(t)$ is given explicitly by

$$\tilde{x}(t) = \int_{\tau_m}^{\infty} x(t-u)g(u)du \equiv \int_{-\infty}^{t-\tau_m} x(u)g(t-u)du, \tag{8.2}$$

τ_m is the minimal maturation delay; and $g(\tau)$ is the density of the distribution of maturation delays as specified below in Section 8.4.2. Since $g(\tau)$ is a density, it is normalized by definition:

$$\int_0^{\infty} g(u)du = 1. \tag{8.3}$$

To completely specify the semidynamical system described by equations (8.1) and (8.2), we must additionally give an initial function

$$x(t') \equiv \varphi(t') \qquad \text{for} \qquad t' \in (-\infty, 0). \tag{8.4}$$

Distribution of Maturation Times. A wide variety of analytic forms could be used for the density of the distribution of the maturation times in the bone marrow. We have chosen to use the density of the gamma distribution

$$g(\tau) = \begin{cases} 0, & \tau \leq \tau_m, \\ \frac{a^{m+1}}{\Gamma(m+1)}(\tau-\tau_m)^m e^{-a(\tau-\tau_m)}, & \tau_m < \tau, \end{cases} \tag{8.5}$$

with $a, m \geq 0$, considered before (Blythe et al. 1984; Cooke and Grossman 1982; Gatica and Waltman 1988; Gatica and Waltman 1982) in a different

context. This choice was predicated on two issues. First, we have found (see Section 8.4.2) that we can achieve a good fit of the existing data on cellular maturation times using equation (8.5). Secondly, the density of the gamma distribution has been used a number of times in the past (Kendall 1948; Powell 1955; Powell 1958) to fit distributions of cell cycle times. When the parameter m in equation (8.5) is a nonnegative integer, then the corresponding equations (8.1) and (8.2) reduce to a system of linear ordinary differential equations coupled to a single nonlinear delayed equation with a discrete (not continuously distributed) delay (Fargue 1973; Fargue 1974; MacDonald 1989). This leads to analytic simplifications, though we do not use them here, since we have typically found noninteger values for the parameter m. We did, however, use this reduction to test the accuracy of our numerical simulations of the full model.

The parameters m, a, and τ_m in the density of the gamma distribution can be related to certain easily determined statistical quantities. The average of the *unshifted* density is given by

$$\tau_2 = \int_{\tau_m}^{\infty} \tau g(\tau) d\tau = \frac{m+1}{a}, \tag{8.6}$$

and thus the average maturation delay as calculated from equation (8.5) is given by

$$\langle \tau \rangle = \tau_m + \tau_2 = \tau_m + \frac{m+1}{a}. \tag{8.7}$$

The variance (denoted by σ^2) is given by

$$\sigma^2 = \frac{m+1}{a^2}. \tag{8.8}$$

Given the expressions (8.6), (8.7), and (8.8) in terms of the gamma distribution parameters m and a, we may easily solve for these parameters in terms of τ_2 and σ^2 to give

$$a = \frac{\tau_2}{\sigma^2} \tag{8.9}$$

and

$$m + 1 = \frac{\tau_2^2}{\sigma^2}. \tag{8.10}$$

Parameter Estimation. Several studies have shown that labeled neutrophils disappear from the circulation with a half-life $t_{1/2}$ of about 7.6 hours in humans (Dancey et al. 1976) and dogs (Deubelbeiss et al. 1975) with a range of 7 to 10 hours. Furthermore, this disappearance rate is unaffected in human (Guerry et al. 1973) and canine cyclical neutropenia (Dale et al. 1972) and is not altered by the administration of exogenous granulocyte colony stimulating factor (Price et al. 1996). Since the decay

coefficient α of equation (8.1) is related to $t_{1/2}$ through the relation

$$\alpha = \frac{\ln 2}{t_{1/2}}, \tag{8.11}$$

we have taken values of $\alpha \in [1.7, 2.4]$ (days^{-1}) in all of the numerical work reported here.

Distributions of maturation times were determined from published data on the emergence of the number of labeled circulating neutrophils following pulse labeling by tritiated thymidine. The published graphed data were scanned and the postscript file viewed with `Ghostview`. `Ghostview` gives coordinates for the position of the points, which, using position of the axes, can be easily transformed to give the actual data points. The data were adjusted for the random death occurring at a rate α by using the method of Dancey, Deubelbeiss, Harker, and Finch (1976).

Assume that the neutrophils spend a period of time u in the bone marrow, and y in the blood. Then the fraction, $N(t)$, of labeled cells in the blood at time t is the probability that the time in the marrow is less than t and that the total time in the marrow and blood before death is greater than t. Let $g(u)$ be the density of the distribution of the maturation times in the marrow, and remember that $g(u)$ is the quantity that we wish to determine. Further note that because of the experimentally observed random destruction of neutrophils in the circulation, if the rate of random destruction is α, then the density of the distribution of destruction rates is given by $\alpha e^{-\alpha y}$. With these observations, for $N(t)$ we finally have

$$N(t) = \int_0^t \int_{t-u}^{\infty} \alpha e^{-\alpha y} g(u) dy\, du = \int_0^t e^{-\alpha(t-u)} g(u) du. \tag{8.12}$$

Thus,

$$e^{\alpha t} N(t) = \int_0^t e^{\alpha u} g(u) du, \tag{8.13}$$

and differentiating both sides with respect to t gives

$$\alpha e^{\alpha t} N(t) + e^{\alpha t} N'(t) = e^{\alpha t} g(t). \tag{8.14}$$

The final result for the density of marrow transit times is

$$g(t) = \alpha N(t) + N'(t). \tag{8.15}$$

Since we had discrete data points from the labeling data, we used the midpoint of two data points and the slope of the joining line in equation (8.15), and determined $g(t)$ at the midpoint. The mean and variance were calculated from the new density, and the corresponding m and a determined from equations (8.9) and (8.10) were used as the initial values in a nonlinear least squares fit to the data. The results of these determinations for a number of published data sets are summarized in Table 8.1. Figure 8.6

Condition	$\langle\tau\rangle$	σ^2	τ_m	*Ref*	a	m
Normal Human	9.70	16.20	3.8	$*$	0.36	1.15
CN Human	7.57	12.01	1.2	♣	0.53	2.38
30 μg G-CSF Human	6.27	4.60	2.4	♢	0.84	2.26
300 μg GCSF Human	4.86	2.30	2.0	♢	1.24	2.56
Normal Dog	3.68	.198	3.0	♡	3.43	1.34
Gray Collie Apogee	3.21	0.042	2.6	♠	14.52	7.86
Gray Collie Nadir	3.42	0.157	2.6	♠	5.22	3.28

Table 8.1. Distribution of maturation time parameters deduced from published data. The units of $\langle\tau\rangle$ and τ_m are in days, σ^2 is in days^2, and a is in days^{-1}. For the references, $*$ = Perry et al. (1966), ♣ =Guerry et al. (1973), ♢ = Price et al. (1996), ♡ = Deubelbeiss et al. (1975), and ♠ = Patt et al. (1973). See the text for details.

shows the raw data as well as the fits to the data using the density of the gamma distribution.

The Steady State and Stability

The Steady State. The equilibrium solution for the functional differential equation (8.1)–(8.2) occurs when

$$\frac{dx}{dt} = 0 = -\alpha x + \mathcal{M}_o(\tilde{x}), \tag{8.16}$$

so the steady state x^* is defined implicitly by the solution of the equation

$$\alpha x^* = \mathcal{M}_o(x^*). \tag{8.17}$$

Given the presumptive monotone decreasing nature of the negative feedback production rate inferred from the biology, there can be but a unique value for the steady-state white blood cell density x^*. It is important to note that x^* is independent of the distribution of the maturation times. However, the stability of x^* is dependent on the density $g(\tau)$, as we now show.

Stability. One of the primary considerations of this section has to do with the stability of the unique steady state, defined implicitly by equation (8.17), and how that stability may be lost. We examine the stability of x^* in the face of very small deviations away from the steady state. Though the mathematical development may seem much different in this model, it is fundamentally the same as the procedure for examining the stability of steady states in ordinary differential equations.

Throughout this analysis, an important parameter that will appear is the *slope* of the production function $\mathcal{M}_o$ evaluated at the steady state, denoted by $\mathcal{M}'_{o*}$. Because of our arguments concerning the negative feedback nature of the peripheral control mechanisms acting on neutrophil production, we know that this slope must be nonpositive (i.e., negative or zero).

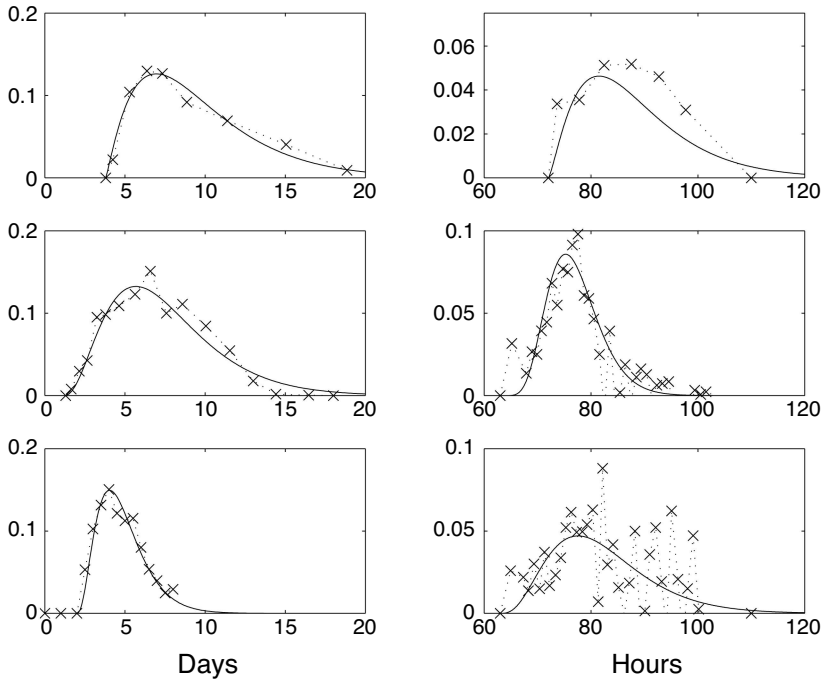

Figure 8.6. Densities of distributions of maturation times and the least square fits to the data achieved using the density of the gamma distribution. The three left-hand panels are for humans and show, from top to bottom, a normal human, data from a cyclical neutropenia patient, and a normal human receiving 300 μg granulocyte colony stimulating factor. The three right-hand panels are for dogs and correspond to (top to bottom) a normal dog, a grey collie at the apogee of the cycle, and a grey collie at the nadir of the cycle. See Table 8.1 for the parameters used to fit the data and the references for the source of the data. From Hearn, Haurie, and Mackey (1998).

To examine the local stability, we write out equation (8.1) for small deviations of x from x^*. In the first (linear) approximation this gives

$$\frac{dx}{dt} \approx -\alpha x + \mathcal{M}_{o*} + (\tilde{x} - x^*)\mathcal{M}'_{o*}, \tag{8.18}$$

wherein

$$\mathcal{M}_{o*} \equiv \mathcal{M}_o(\tilde{x} = x^*) \tag{8.19}$$

and

$$\mathcal{M}'_{o*} \equiv \frac{d\mathcal{M}_o(\tilde{x})}{d\tilde{x}}|_{\tilde{x}=x^*}. \tag{8.20}$$

Utilizing equation (8.17) and defining the deviation from equilibrium as $z(t) = x(t) - x^*$, we can rewrite equation (8.18) in the form

$$\frac{dz}{dt} = -\alpha z + \mathcal{M}'_{o*} \int_{-\infty}^{t-\tau_m} z(u) g(t-u) du. \tag{8.21}$$

As before, we assume that the deviation z from the steady state has the form $z(t) \bowtie \exp(\lambda t)$, substitute this into equation (8.21), carry out the indicated integrations, and finally obtain

$$\lambda + \alpha = \mathcal{M}'_{o*} \left(\frac{a}{\lambda + a} \right)^{m+1} e^{-\lambda \tau_m}. \tag{8.22}$$

Equation (8.22) for the eigenvalues λ may have a variety of solutions. If an eigenvalue λ is real, then a simple graphical argument shows that the eigenvalue will be negative and contained in the open interval $(-\alpha, -a)$.

Alternatively, the eigenvalue solutions of equation (8.22) may be complex conjugate numbers, in which case, as seen before, the most interesting thing to know is when the real part of the eigenvalue is identically zero. This will define the boundary between a locally stable steady state when Re $\lambda < 0$ and a locally unstable steady state with Re $\lambda > 0$.

To investigate this possibility, we take $\lambda = \mu + i\omega$ and substitute this into equation (8.22) to give, with $\mu = 0$,

$$i\omega + \alpha = \mathcal{M}'_{o*} \left(\frac{a}{i\omega + a} \right)^{m+1} e^{-i\omega \tau_m}, \tag{8.23}$$

or rewriting,

$$\left[(i\omega + \alpha) \left(1 + i \frac{\omega}{a} \right)^{m+1} \right] = \mathcal{M}'_{o*} e^{-i\omega \tau_m}. \tag{8.24}$$

This equation can be manipulated to give a set of parametric equations in α and $\mathcal{M}'_{o*}$. We start by setting

$$\tan \theta = \frac{\omega}{a}. \tag{8.25}$$

Using de Moivre's formula in equation (8.24) gives

$$\begin{aligned} (\alpha + i\omega)(\cos[(m+1)\theta]) + i \sin[(m+1)\theta]) = \\ \mathcal{M}'_{o*} \cos^{m+1} \theta (\cos \omega \tau_m - i \sin \omega \tau_m). \end{aligned} \tag{8.26}$$

Equating the real and imaginary parts of equation (8.26) gives the coupled equations

$$\alpha - \mathcal{M}'_{o*} R \cos \omega \tau_m = \omega \tan[(m+1)\theta] \tag{8.27}$$

and

$$\alpha \tan[(m+1)\theta] + \mathcal{M}'_{o*} R \sin \omega \tau_m = -\omega, \tag{8.28}$$

where

$$R = \frac{\cos^{m+1}\theta}{\cos[(m+1)\theta]}. \tag{8.29}$$

Equations (8.27) and (8.28) are easily solved for α and $\mathcal{M}'_{o*}$ as parametric functions of ω to give

$$\alpha(\omega) = -\frac{\omega}{\tan[\omega\tau_m + (m+1)\tan^{-1}(\omega/a)]} \tag{8.30}$$

and

$$\mathcal{M}'_{o*}(\omega) = -\frac{\omega}{\cos^{m+1}[\tan^{-1}(\omega/a)]\sin[\omega\tau_m + (m+1)\tan^{-1}(\omega/a)]}. \tag{8.31}$$

To show that the stability boundary defined implicitly by equations (8.30) and (8.31) delimits a transition from a locally stable steady state to a locally unstable steady state as $\mathcal{M}'_{o*}$ decreases, we must show that the real part of the eigenvalue is negative on one side of the boundary and positive on the other. Thus, the real part of $d\lambda/d\mathcal{M}'_{o*}$, or equivalently of $(d\lambda/d\mathcal{M}'_{o*})^{-1}$, must be negative when $\lambda = i\omega$.

Implicit differentiation of equation (8.22) yields

$$\left(\frac{d\lambda}{d\mathcal{M}'_{o*}}\right)^{-1} = \left(\frac{\lambda+a}{a}\right)^{m+1} e^{\lambda\tau_m} + \mathcal{M}'_{o*}\frac{m+1}{\lambda+a} + \mathcal{M}'_{o*}\tau_m, \tag{8.32}$$

and the use of equation (8.22) in (8.32) gives

$$\left(\frac{d\lambda}{d\mathcal{M}'_{o*}}\right)^{-1} = \mathcal{M}'_{o*}\left(\frac{1}{\lambda+\alpha} + \frac{m+1}{\lambda+a} + \tau_m\right). \tag{8.33}$$

Evaluating (8.33) at $\lambda = i\omega$ and eliminating complex numbers in the denominators, we have

$$\left(\frac{d\lambda}{d\mathcal{M}'_{o*}}\right)^{-1} = \mathcal{M}'_{o*}\left(\frac{\alpha - i\omega}{\alpha^2+\omega^2} + \frac{(m+1)(a-i\omega)}{a^2+\omega^2} + \tau_m\right), \tag{8.34}$$

with

$$Re\left(\left(\frac{d\lambda}{d\mathcal{M}'_{o*}}\right)^{-1}\right) = \mathcal{M}'_{o*}\left(\frac{\alpha}{\alpha^2+\omega^2} + \frac{(m+1)a}{a^2+\omega^2} + \tau_m\right). \tag{8.35}$$

If $\mathcal{M}'_{o*}$ is negative (as in our case), then the right-hand side of equation (8.35) is negative, indicating that for increases in $\mathcal{M}'_{o*}$ to more positive values at the boundary where $\mu \equiv 0$, the real part of the eigenvalue λ is crossing from positive to negative.

Thus, we conclude that the locus of points defined by equations (8.30) and (8.31) defines the location in $(\alpha, \mathcal{M}'_{o*})$ parameter space where a supercritical Hopf bifurcation takes place and a periodic solution of period

$$T_{\text{Hopf}} = \frac{2\pi}{\omega} \tag{8.36}$$

occurs.

Implications of the Local Stability Analysis

In Figure 8.7 we have parametrically plotted $\mathcal{M}'_{o*}(\omega)$ versus $\alpha(\omega)$ (ω is the parameter) [equations (8.30) and (8.31)] to give the stability boundaries for a normal human and a human with cyclical neutropenia using the data of Table 8.1. (Ignore the lines corresponding to G-CSF for the time being). The two vertical dashed lines correspond to the normal range of α values as discussed in Section 8.4.2; the lower dashed line is the stability boundary for the cyclical neutropenia case, and the solid line is for the normal human. Regions above a given stability boundary in $(\alpha, \mathcal{M}'_{o*})$ parameter space correspond to a locally stable steady-state neutrophil level, while regions below are unstable. For values of $(\alpha, \mathcal{M}'_{o*})$ exactly on a given line there is a bifurcation to a periodic solution with Hopf period T_{Hopf} as discussed above.

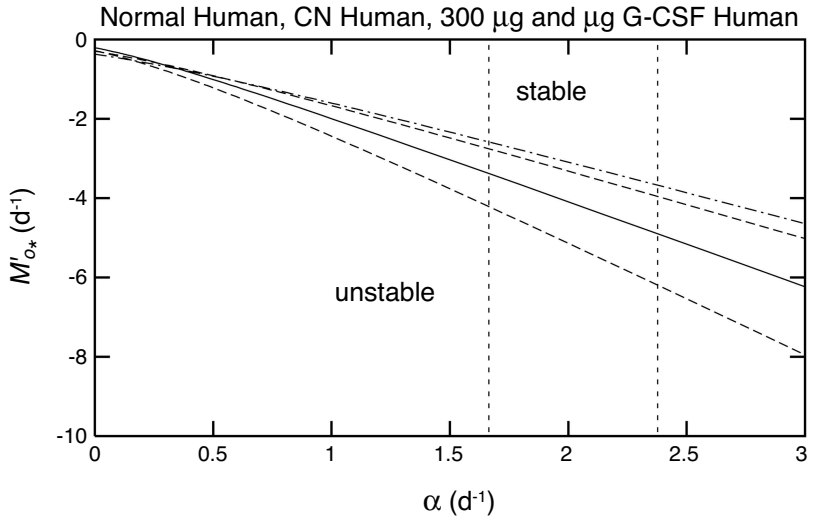

Figure 8.7. A parametric plot of the regions of linear stability and instability based on data for normal humans (solid line) (Perry et al. 1966), humans with cyclical neutropenia (CN) (lower dashed line) (Guerry et al. 1973), and normal humans administered granulocyte colony stimulating factor (G-CSF) (upper dashed line is for 30 μg, and the dash–dot line is for 300 μg) (Price et al. 1996). In this and all subsequent stability diagrams, points $(\alpha, \mathcal{M}'_{o*})$ above a given stability line correspond to linear stability of the steady state, and those below correspond to an unstable steady state. See the text for details. From Hearn, Haurie, and Mackey (1998).

Implications for the Origin of Cyclical Neutropenia. The first point to be noted is the following: If the model for granulopoiesis is stable for a normal human, then a simple alteration of the characteristics of the maturation time distribution to correspond to the value for cyclical neutropenia

(Table 8.1) is incapable of singlehandedly inducing an instability. Furthermore, note that the unique steady state of the model as given implicitly by equation (8.17) is *independent* of any alterations in the distribution of maturation times. However, the dynamically varying neutrophil levels in cyclical neutropenia are often depressed relative to the normal state (Section 8.3.2), thus implying that a simple alteration of the distribution of maturation times could not be the sole source of cyclical neutropenia dynamics alone.

Examination of Figure 8.7 shows that if the dynamic behavior of cyclical neutropenia is to be a result of an instability in this model, then in addition to the known alterations in the distribution of maturation times, there must be a concomitant decrease in $\mathcal{M}'_{o*}$ to more negative values such that $(\alpha, \mathcal{M}'_{o*})$ falls in the zone of parameter space where x^* is unstable. Since one of the hallmarks of cyclical neutropenia is an oscillation about a reduced average neutrophil count, this decrease in $\mathcal{M}'_{o*}$ must also be accompanied by a decrease in $\mathcal{M}_{o*}$ to account for the decrease in x^*. (Remember that α is not altered in cyclical neutropenia, so an increase in α cannot be the source of these depressed levels.)

Suppose that in humans such a decrease in $\mathcal{M}'_{o*}$ has taken place, i.e., that $\mathcal{M}'_{o*}$ has become sufficiently negative for an unstable situation to occur. We can calculate exactly the period of the solution when the Hopf bifurcation to unstable behavior occurs. In the case of the g parameters for the normal human, we have $T_{\text{Hopf}} \in [18.2, 17.8]$ days for $\alpha \in [1.7, 2.4]$. The corresponding range for the cyclical neutropenia boundary is $T_{\text{Hopf}} \in [14.2, 13.8]$ days. These values are lower than the smallest observed periods in clinical cyclical neutropenia as reviewed in Section 8.3.2 and as found in the analysis of Haurie, Mackey, and Dale (1999).

Turning to the case of canine cyclical neutropenia, we have plotted stability boundaries for a normal dog and grey collies at the peak and nadir of their cycle in Figure 8.8. The stability boundaries for all three situations (using the appropriate parameters from Table 8.1) fall virtually on top of one another. As with human cyclical neutropenia, the local stability analysis suggests that in contrast with the hypothesis of Schmitz, Loeffler, Jones, Lange, and Wichmann (1990), the origin of canine cyclical neutropenia is not a consequence of alterations in the distribution of marrow maturation times for neutrophil precursors alone. Rather, as in the human case, a shift in $\mathcal{M}'_{o*}$ to more negative values would be required to effect the requisite instability.

Assume for the grey collie that such a shift in $\mathcal{M}'_{o*}$ to values sufficiently negative to destabilize the system has taken place. What, then, are the predicted Hopf periods at the onset of the ensuing oscillation? Based on the data for normal dogs presented in Table 8.1, for $\alpha \in [1.7, 2.4]$ the local stability analysis of Section 8.4.2 predicts that $T_{\text{Hopf}} \in [8.5, 8.2]$ days. For the grey collie maturation distribution data taken at the nadir of the cycle this range is reduced to $T_{\text{Hopf}} \in [8.0, 7.6]$ days, while the collie data from

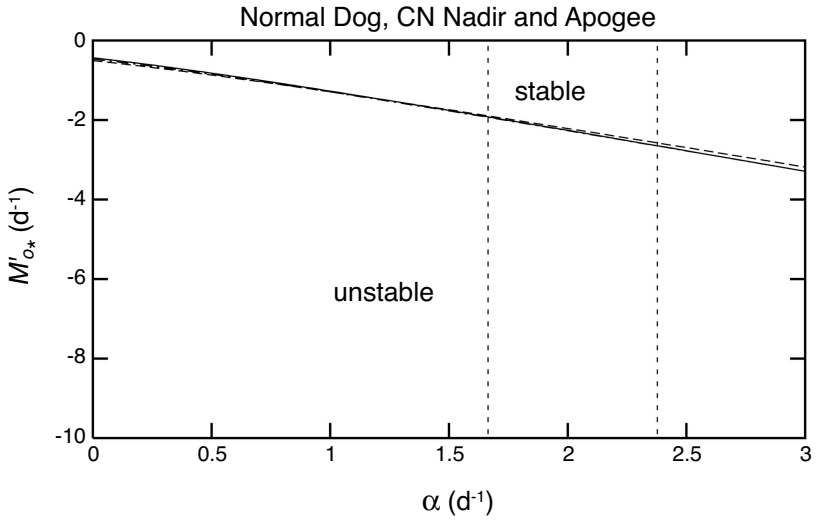

Figure 8.8. A parametric plot of the regions of linear stability and instability based on data for normal dogs taken from Deubelbeiss, Dancey, Harker, and Finch (1975) and from grey collies at the apogee and nadir of their oscillation as taken from Patt, Lund, and Maloney (1973). Note that the three stability boundaries are virtually indistinguishable from one another. CN = cyclical neutropenia. From Hearn, Haurie, and Mackey (1998).

the apogee predicts $T_{\text{Hopf}} \in [7.4, 7.1]$ days. All of these estimates are below the reported ranges for the period of canine cyclical neutropenia discussed in Section 8.3.2 and in Haurie, Person, Mackey, and Dale (1999).

Thus, for both human and grey collie cyclical neutropenia we conclude that there is no evidence from the linear stability analysis that the dynamics of cyclical neutropenia are due to an instability in the peripheral control of granulopoiesis caused by a change in the distribution of cell maturation times.

Assessing the Effects of Granulocyte Colony Stimulating Factor. The second point that we can address with the aid of the local stability analysis of Section 8.4.2 is the effect of granulocyte colony stimulating factor on the stability of the system in normal humans. In Figure 8.7 we have plotted the stability boundaries for the data of Table 8.1 corresponding to the alterations in normal humans induced by 30 μg and 300 μg granulocyte colony stimulating factor reported by Price, Chatta, and Dale (1996). (Note that if the individuals in this study weighed 70 kg, then the dosage was either 0.43 μg/kg–day or 4.3 μg/kg–day, respectively.) It is clear from Figure 8.7 that the region of parameter space in which the normal human control system is stable is actually *decreased* by the administration of granulocyte colony stimulating factor, since the stability boundaries for both dosages of granulocyte colony stimulating factor lie above the stability boundary for

a normal human. Unfortunately, we have been unable to locate any data for the effects of granulocyte colony stimulating factor on the density g of the distribution of maturation times in dogs, but based on the comparable data for humans we would not expect large quantitative differences.

If data were available for the effects of the granulocyte colony stimulating factor on the density of the distribution of maturation times in humans with cyclical neutropenia, we could assess the potential role of the granulocyte colony stimulating factor in altering the period as noted in the clinical literature. However, we must note that if the changes induced by the granulocyte colony stimulating factor in cyclical neutropenia are comparatively similar to those in normals, then it is unlikely that the granulocyte colony stimulating factor could ever act to stabilize a peripheral instability in neutrophil numbers, since its role seems to be a destabilizing one.

Discussion and Conclusions

Our original motivation in carrying out the analysis presented here was to examine the hypothesis that cyclical neutropenia was due to a loss of stability in the peripheral control of neutrophil production. Based on the considerations of Section 8.4.2 that are independent of the precise nature of the control function assumed, we conclude that any alterations of parameters in this peripheral control system consistent with the extant laboratory and clinical data on cyclical neutropenia are unable to reproduce either the characteristics of clinical cyclical neutropenia or its laboratory counterpart in the grey collie. Further, we conclude that the dynamic effects of granulocyte colony stimulating factor treatment of cyclical neutropenia are probably not primarily due to the alterations of the peripheral control dynamics.

Rather, we conclude that the dynamics of cyclical neutropenia are due to a destabilization of the hematopoietic stem cell population as originally proposed by Mackey (1978) and Mackey (1979).

8.5 Stem Cell Dynamics and Cyclical Neutropenia

In trying to understand and model the properties of cyclical neutropenia as discussed in Section 8.3.2, one of the most crucial clues is the observation of the effect of continuous cyclophosphamide and busulfan administration in normal dogs (Morley and Stohlman 1970; Morley et al. 1970). Though in most animals these drugs led to a pancytopenia whose severity was proportional to the drug dose, in some dogs low doses led to a mild pancytopenia, intermediate doses gave a cyclical neutropenia-like behavior with a period between 11 and 17 days, and high drug levels led either to death or gross pancytopenia. When the cyclical neutropenia-like behavior occurred it was at circulating white blood cell levels of one-half to one-third normal. To this

we must add the observation that patients undergoing hydroxurea therapy sometimes develop cyclical neutropenia-like symptoms (Kennedy 1970), as do patients receiving cyclophosphamide (Dale et al. 1973).

Both cyclophosphamide and busulfan selectively kill cells within the DNA synthetic phase of the cell cycle, and the fact that both drugs are capable of inducing cyclical neutropenia-like behavior strongly suggest that the origin of cyclical neutropenia as a disease is due to an abnormally large death rate (apoptosis) in the proliferative phase of the cell cycle of a population of cells – the hematopoietic stem cells – more primitive than the granulocyte/monocyte colony forming units, CFU-GM, and the erythrocytic burst forming units, BFU-E. Here we interpret the effects of an increase in the rate of irreversible apoptotic loss from the proliferating phase of the hematopoietic stem cells (γ in Figure 8.9) on blood cell production (Mackey 1978).

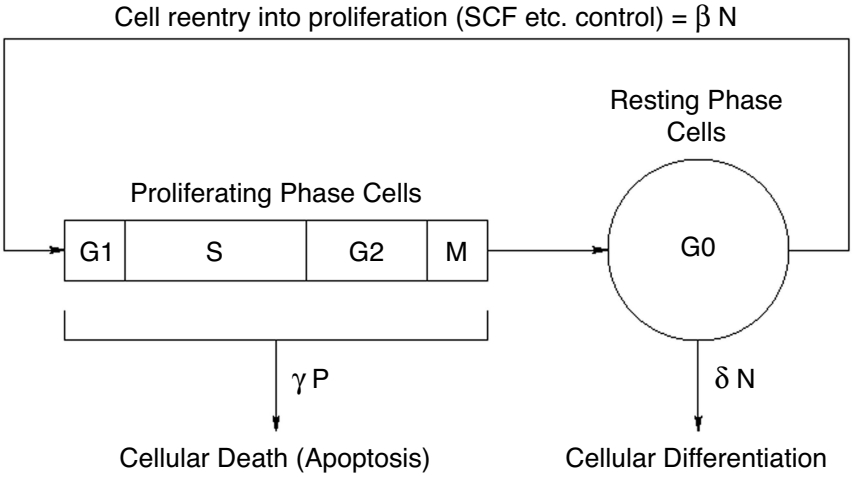

Figure 8.9. A schematic representation of the control of hematopoietic stem cell regeneration. Proliferating phase cells (P) include those cells in G_1, S (DNA synthesis), G_2, and M (mitosis), while the resting phase (N) cells are in the G_0 phase. Local regulatory influences are exerted via a cell-number-dependent variation in the fraction of circulating cells, δ is the **normal** rate of differentiation into all of the committed stem cell populations, while γ represents a loss of proliferating phase cells due to apoptosis. See Mackey (1978), Mackey (1979) for further details.

The dynamics of this hematopoietic stem cell population are governed (Mackey 1978; Mackey 1979) by the pair of coupled differential delay equations

$$\frac{dP}{dt} = -\gamma P + \beta(N)N - e^{-\gamma\tau}\beta(N_\tau)N_\tau \tag{8.37}$$

and

$$\frac{dN}{dt} = -[\beta(N) + \delta]N + 2e^{-\gamma\tau}\beta(N_\tau)N_\tau, \tag{8.38}$$

where τ is the time required for a cell to traverse the proliferative phase, and the resting to proliferative phase feedback rate β is taken to be

$$\beta(N) = \frac{\beta_0\theta^n}{\theta^n + N^n}. \tag{8.39}$$

An examination of equation (8.38) shows that this equation could be interpreted as describing the control of a population with a delayed mixed feedback-type production term $[2e^{-\gamma\tau}\beta(N_\tau)N_\tau]$ and a destruction rate $[\beta(N) + \delta]$ that is a decreasing function of N.

This model has two possible steady states. There is a steady state corresponding to no cells, $(P_1^*, N_1^*) = (0, 0)$, which is stable if it is the only steady state and which becomes unstable whenever the second positive steady state (P_2^*, N_2^*) exists.

The stability of the nonzero steady state depends on the value of γ. When $\gamma = 0$, this steady state cannot be destabilized to produce dynamics characteristic of cyclical neutropenia. On the other hand, for $\gamma > 0$, increases in γ lead to a decrease in the hematopoietic stem cell numbers and a consequent decrease in the cellular efflux (given by δN) into the differentiated cell lines. This diminished efflux becomes unstable when a critical value of γ is reached, $\gamma = \gamma_{\text{crit},1}$, at which a supercritical Hopf bifurcation occurs. For all values of γ satisfying $\gamma_{\text{crit},1} < \gamma < \gamma_{\text{crit},2}$, there is a periodic solution of equation (8.38) whose period is in good agreement with that seen in cyclical neutropenia. At $\gamma = \gamma_{\text{crit},2}$, a reverse bifurcation occurs and the greatly diminished hematopoietic stem cell numbers as well as cellular efflux again becomes stable. All of these properties are illustrated in Figure 8.10.

Separate estimations of the parameter sets for human and grey collie hematopoietic stem cell populations give predictions of the period of the oscillation at the Hopf bifurcation that are consistent with those observed clinically and in the laboratory.

Numerical simulations, shown in Figures 8.11 and 8.12, of equations (8.37) and (8.38) bear out the results of the above local stability analyses. As expected, an increase in γ is accompanied by a decrease in the average number of circulating cells. For certain values of γ an oscillation appears. Over the range of γ in which an oscillation occurs, the period increases as γ increases. However, the amplitude of the oscillation first increases and then decreases. (Similar observations hold for the model of autoimmune hemolytic anemia as the control parameter γ is increased.) When all the parameters in the model are set to the values estimated from laboratory and clinical data, no other types of bifurcations are found. Although these simulations also indicate the existence of multiple bifurcations and chaotic behaviors, these more complex dynamics are observed only for

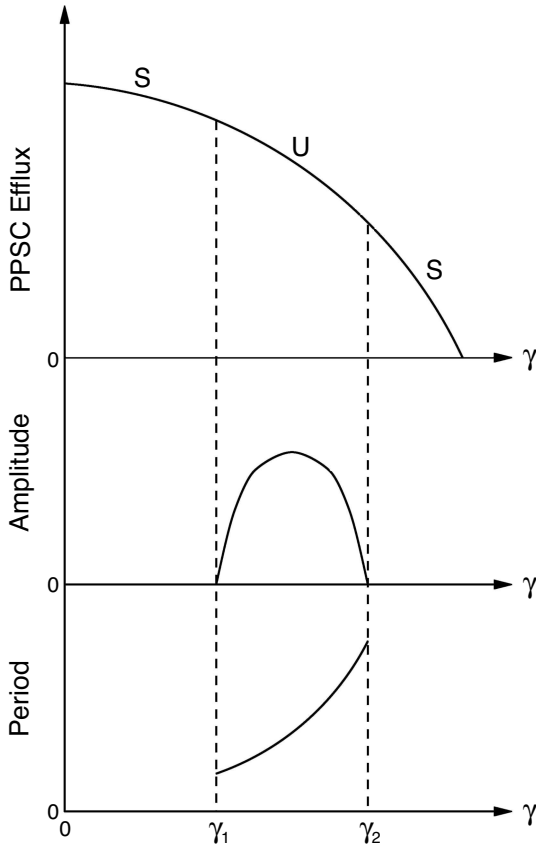

Figure 8.10. Schematic representation of the combined analytic and numerically determined stability properties of the hematopoietic stem cell model. See the text for details. From Mackey (1996).

nonphysiological choices of the parameters. Thus the observed irregularities in the fluctuations in blood cell numbers in cyclical neutropenia cannot be related to chaotic solutions of equation (8.38). These results suggest that cyclical neutropenia is likely related to defects, possibly genetic, within the hematopoietic stem cell population that lead to an abnormal ($\gamma > 0$) apoptotic loss of cells from the proliferative phase of the cell cycle.

8.5.1 Understanding Effects of Granulocyte Colony Stimulating Factor in Cyclical Neutropenia

Recent clinical and experimental work has focused on the modification of the symptoms of hematological disorders, including periodic hematopoiesis, by the use of various synthetically produced cytokines (Sachs 1993; Sachs

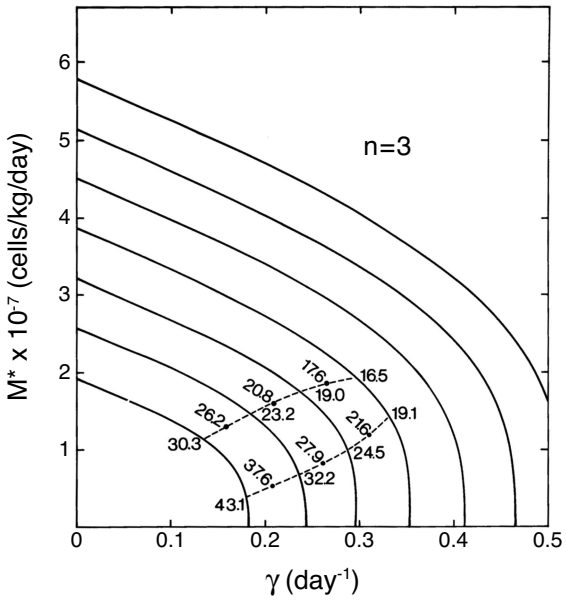

Figure 8.11. Variation of the total cellular differentiation efflux (δN) as a function of the apoptotic death rate γ from the proliferating cell population in humans ($n = 3$). Parameters in the model were estimated assuming a proliferating fraction of 0.1, and an amplification of 16 in the recognizable erythroid, myeloid, and megakaryocytic precursors populations. See Mackey (1978), Mackey (1979) for details. The hematopoietic stem cell parameters corresponding to each curve from the top down are $(\delta, \beta_0, \tau, \theta \times 10^{-8}) = (0.09,\ 1.58,\ 1.23,\ 2.52)$, (0.08, 1.62, 1.39, 2.40), (0.07, 1.66, 1.59, 2.27), (0.06, 1.71, 1.85, 2.13), (0.05, 1.77, 2.22, 1.98), (0.04, 1.84, 2.78, 1.81), and (0.03, 1.91, 3.70, 1.62) in units (days^{-1}, days^{-1}, days, cells/kg). The dashed solid lines indicate the boundaries along which stability is lost in the linearized analysis, and the numbers indicate the predicted (Hopf) period (in days) of the oscillation at the Hopf bifurcation. From Mackey (1978).

and Lotem 1994; Cebon and Layton 1984), e.g., the recombinant colony stimulating factors rG-CSF and rGM-CSF, whose receptor biology is reviewed in (Rapoport et al. 1992), and Interlukin-3. These cytokines are now known to interfere with the process of apoptosis or to lead to a decrease in γ within the context of the hematopoietic stem cell model of Section 8.5.

Human colony stimulating factors increase both the numbers and proliferation rate of white blood cell precursors in a variety of situations (Bronchud et al. 1987; Lord et al. 1989; Lord et al. 1991). Furthermore, colony stimulating factor in mice is able to stimulate replication in both stem cells and early erythroid cells (Metcalf et al. 1980).

It is known that in aplastic anemia and cyclical neutropenia there is an inverse relationship between plasma levels of granulocyte colony stimulating factor and white blood cell numbers (Watari et al. 1989). Further, it has

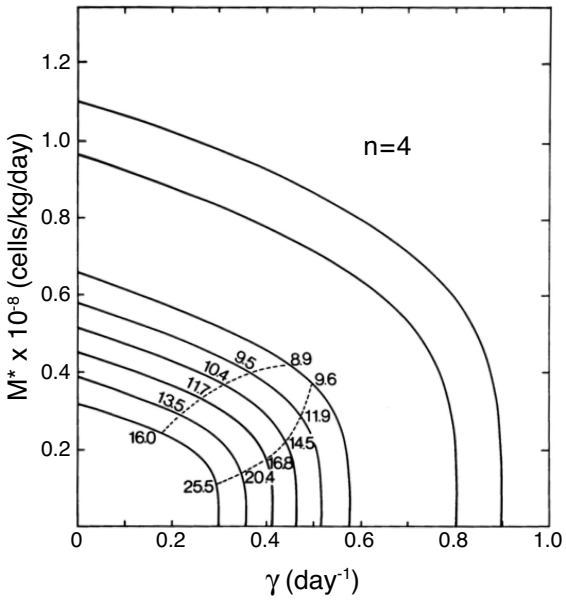

Figure 8.12. As in Figure 8.11, but all calculations done with parameters appropriate for dogs. Reproduced from Mackey (1978).

been shown (Layton et al. 1989) that the $t_{1/2}$ of the granulocyte colony stimulating factor in the circulation is short, on the order of 1.3 to 4.2 hours, so the dynamics of the destruction of the granulocyte colony stimulating factor are unlikely to have a major role in the genesis of the dynamics of cyclical neutropenia.

In the grey collie it has been shown that at relatively low doses of the granulocyte colony stimulating factor the mean white blood cell count is elevated (from 10 to 20 times), as is the amplitude of the oscillations (Hammond et al. 1990), while higher dosages (Lothrop et al. 1988; Hammond et al. 1990) lead to even higher mean white blood cell numbers but eliminate the cycling. Another interesting observation is that in the collie, granulocyte colony stimulating factor administration results in a decrease in the period of the peripheral oscillation. The elevation of the mean white blood cell levels and the amplitude of the oscillations, as well as an enhancement of the oscillations of platelets and reticulocytes, at low levels of the granulocyte colony stimulating factor has also been reported in humans (Hammond et al. 1990; Migliaccio et al. 1990; Wright et al. 1994), and it has been also noted that the fall in period observed in the collie after granulocyte colony stimulating factor administration occurs in humans with a fall in period from 21 to about 14 days. Finally, it should be mentioned that treatment with granulocyte colony stimulating factor in patients with agranulocytosis has also lead to a significant increase in the mean white blood cell counts

and, in some patients, to the induction of white blood cell oscillations with periods ranging from 7 to 16 days.

Our major clue to the nature of the effects of the granulocyte colony stimulating factor comes from its prevention of apoptosis, and the work of Avalos et al. (1994), who have shown in dogs that there is no demonstrable alteration in the number, binding affinity, or size of the granulocyte colony stimulating factor receptor on cyclical neutropenia dogs as compared to normal dogs. They thus conclude that cyclical neutropenia "is caused by a defect in the granulocyte colony stimulating factor signal transduction pathway at a point distal to the granulocyte colony stimulating factor binding ... ." The data of Avalos et al. (1994) can be used to estimate that

$$\gamma_{\max}^{\mathrm{CN}} \approx 7 \times \gamma_{\max}^{\mathrm{norm}}. \tag{8.40}$$

The results of Hammond, Chatta, Andrews, and Dale (1992) in humans are consistent with these results in dogs.

Less is known about the effect of the granulocyte/monocyte colony stimuling factor, GM-CSF, but it is known that administration of GM-CSF in humans gives an elevation of the mean white blood cell level but only by relatively modest amounts, 1.5 to 3.9 times (Wright et al. 1994), but either dampens the oscillations of cyclical neutropenia or eliminates them entirely. The same effect has been shown (Hammond et al. 1990) in the grey collie. It is unclear whether the period of the peripheral cell oscillations has a concomitant decrease, as is found with the granulocyte colony stimulating factor. The abnormal responsiveness of precursors to granulocyte colony stimulating factor in grey collies and humans with cyclical neutropenia (Hammond et al. 1992; Avalos et al. 1994) is mirrored in the human response to the granulocyte/monocyte colony stimulating factor (Hammond et al. 1992).

Thus, the available laboratory and clinical data on the effects of colony stimulating factors in periodic hematopoiesis indicate that (1) there is extensive intercommunication between all levels of stem cells; and (2) within the language of nonlinear dynamics, colony stimulating factors may be used to titrate the dynamics of periodic hematopoiesis to the point of inducing a reverse Hopf bifurcation (disappearance of the oscillations). In the course of this titration, there may also be a shift in the period.

The behavior in periodic hematopoiesis when colony stimulating factor is administered is qualitatively consistent with the hematopoietic stem cell model discussed in Section 8.5, since it is known that colony stimulating factor interferes with apoptosis, and thus administration of colony stimulating factor is equivalent to a decrease in the apoptotic death rate γ.

8.6 Conclusions

Delayed feedback mechanisms constitute a core element in the regulation of blood cell populations. These delayed feedback mechanisms can produce oscillations whose period typically ranges from 2 to 4 times the delay, but which may be even longer. Thus it is not necessary to search for illusive and mystical entities (Beresford 1988), such as ultradian rhythms, to explain the periodicity of these disorders.

The observations in this chapter emphasize that an intact control mechanism for the regulation of blood cell numbers is capable of producing behaviors ranging from no oscillation to periodic oscillations to more complex irregular fluctuations, i.e., chaos. The type of behavior produced depends on the nature of the feedback, i.e., negative or mixed, and on the value of certain underlying control parameters, e.g., peripheral destruction rates or maturation times. Pathological alterations in these parameters can lead to periodic hematological disorders.

8.7 Computer Exercises: Delay Differential Equations, Erythrocyte Production and Control

Objectives

The purpose of these exercises is to gain some familiarity with the behavior of the solutions of differential delay equations by using both analytical and numerical approaches. We are going to do this within the context of a simple model for erythrocyte production and control. For the numerical work, you will use `XPP`* for these exercises.

A Simple Model for the Regulation of Red Blood Cell Production

Consider the control of erythrocyte, or red blood cell, production as represented schematically in Figure 8.13.

A fall in circulating erythrocyte numbers leads to a decrease in hemoglobin levels and thus in arterial oxygen tension. This decrease in turn triggers the production of renal erythropoietin, which increases the cellular production within the early committed erythrocyte series cells, and thus the cellular efflux from the erythrocytic colony forming unit, CFU-E, into the identifiable proliferating and nonproliferating erythroid precursors,

*See Introduction to `XPP` in Appendix A.

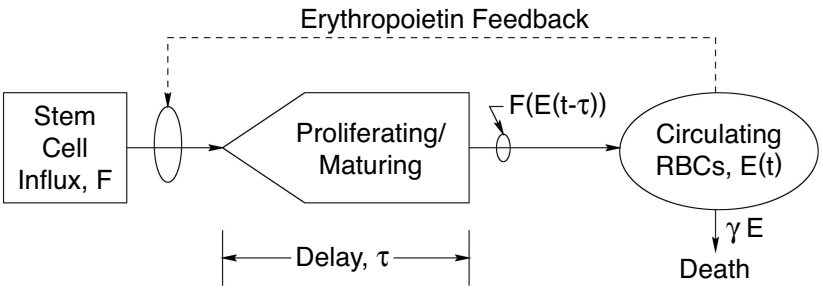

Figure 8.13. A schematic representation of the regulation of red blood cell production. Here the major features and parameters are defined for the simple model that leads to equation (8.41). From Mackey (1996).

and ultimately augments circulating erythrocyte numbers (i.e., negative feedback).

To formulate this sequence of physiological processes in a mathematical model, we let $E(t)$ (cells/kg) be the circulating density of red blood cells as a function of time, β (cells/kg-day) be the stem cell influx under erythropoietin control, τ (days) be the time required to pass through recognizable precursors, and γ (days^{-1}) be the loss rate of red blood cells in the circulation. We can then write the rate of change of erythrocyte numbers as a balance between their production and their destruction:

$$\frac{dE(t)}{dt} = \beta(E(t-\tau)) - \gamma E(t). \tag{8.41}$$

Once a cell from the hematopoietic stem cell compartment is committed to the erythroid series, it undergoes a series of nuclear divisions and enters a maturational phase for a period of time ($\tau \simeq 5.7$ days) before release into the circulation, and the argument in the production function is therefore $E(t-\tau)$, and not $E(t)$. Thus, changes that occur at time t were actually initiated at a time $t-\tau$ in the past. We adopt the usual convention of $E_\tau(t) = E(t-\tau)$, and also do not explicitly denote the time unless necessary. Then the simple model (8.41) for red blood cell dynamics takes the alternative form

$$\frac{dE}{dt} = \beta(E_\tau) - \gamma E. \tag{8.42}$$

To define an appropriate form for the production function β, we use in vivo measurements of erythrocyte production rates in rats and other mammals including humans. The feedback function saturates at low erythrocyte numbers, and is a decreasing function of increasing red blood cell levels. A convenient function that captures this behavior, has sufficient flexibility to be able to fit the data, and is easily handled analytically is given by

$$\beta(E_\tau) = \beta_0 \frac{\theta^n}{E_\tau^n + \theta^n}, \tag{8.43}$$

where β_0 (units of cells/kg-day) is the maximal red blood cell production rate that the body can approach at very low circulating red blood cell numbers, n is a positive exponent, and θ (units of cells/kg) is a parameter. These three parameters have to be determined from experimental data related to red blood cell production rates.

Combining equations (8.42) and (8.43), we have the final form for our model of red blood cell control given as

$$\frac{dE}{dt} = \beta_0 \frac{\theta^n}{E_\tau^n + \theta^n} - \gamma E. \tag{8.44}$$

As discussed in Chapter 9, we have to specify an initial condition in the form of a *function* defined for a period of time equal to the duration of the time delay. Thus we will select

$$E(t') = \phi(t'), \qquad -\tau \le t' \le 0. \tag{8.45}$$

Usually we consider only initial functions that are constant, but it must be noted that some differential delay equations can display multistable behavior in which there are two or more coexisting locally stable solutions, depending on the initial function.

Ex. 8.7-1. A *steady state* (or stationary) solution for the model (8.44) is defined by the requirement that the red blood cell number not be changing with time. This means that

$$E(t) = E(t-\tau) = E_\tau(t) = \text{a constant, the steady state} = E^*, \tag{8.46}$$

and

$$\frac{dE}{dt} = 0 \qquad \text{so} \qquad \beta(E^*) = \beta_0 \frac{\theta^n}{E^{*n} + \theta^n} = \gamma E^*. \tag{8.47}$$

We cannot solve (8.47) to get an analytic form for E^*, but a simple graphical argument shows that there is only one value of E^* satisfying (8.47). This value of the steady state occurs at the intersection of the graph of γE^* with the graph of $\beta(E^*)$.

In this first problem, you must determine the stability of E^* using a linear expansion in (8.44).

a. Expand the function β around E^* to obtain, with $z(t) = E(t) - E^*$, the linear differential delay equation

$$\frac{dz}{dt} = \beta'(E^*) z_\tau - \gamma z. \tag{8.48}$$

b. Assuming that $z(t) \simeq e^{\lambda t}$ in equation (8.48), derive the equation

$$\lambda = \beta'(E^*) e^{-\lambda\tau} - \gamma \tag{8.49}$$

that λ must satisfy.

Letting $\lambda = i\omega$, show that the relation connecting τ, $\beta'(E^*)$, and γ that must be satisfied in order for the eigenvalues to have real part

identically zero is given by

$$\tau = \frac{\cos^{-1}\left(\dfrac{\gamma}{\beta'(E^*)}\right)}{\sqrt{\beta'(E^*)^2 - \gamma^2}}. \tag{8.50}$$

Ex. 8.7-2. In this exercise, you will numerically integrate equation (8.44). In the code written to simulate equation (8.44), the erythrocyte numbers E have been scaled by the numerical value of the parameter θ in the erythropoietin feedback function (8.43), since `XPP` gets very cranky whenever dependent variables exceed 100 in absolute value.

(a) Rewrite equation (8.44) in the dependent variable, and define a new variable $x = E/\theta$ to transform equation (8.44) into

$$\frac{dx}{dt} = \frac{\beta_0}{\theta}\frac{1}{x_\tau^n + 1} - \gamma x. \tag{8.51}$$

The code for equation (8.44) is written in `aiha1.ode`.

(b) Open up `XPP` with the code for equation (8.44) by typing `xppaut aiha1.ode`, and turn off the bell.
The choice of `Method`, which determines the numerical algorithm used to integrate the differential delay equation, is essential. Differential delay equations can be pretty tricky to deal with, and many people have come to grief by using an adaptive step size method to integrate them. (Can you think of why this might happen?) So, we want to make sure that the one that is being used is *not* adaptive. Check that `(R)unge-Kutta x` method is selected.
Having gotten through the above, you are ready to try a numerical simulation.
You should see a periodic variation in the scaled erythrocyte numbers (x) versus time, and this is because γ was picked to be inside the zone of instability of $x^* \equiv E^*/\theta$.
What is the period and amplitude of this periodic variation?

(c) Now you can compare the predictions, from the linear analysis, of the stability boundaries, and at the same time determine qualitatively how the period and amplitude of the oscillatory erythrocyte numbers within the unstable range of γ change as γ is increased.

Use a `(R)ange` of `gamma`, with `Steps: 5` to begin with and the starting and ending values slightly below and above the values of γ_1 and γ_2, respectively, employing different values in an exploratory mode.

Next you can try to change some of the other parameters in the equation to see how they affect the solution behavior, as well as its stability, and see how your intuition matches with what you see numerically. Can you find any values of parameters such that numerically there seems to be a secondary bifurcation?

Ex. 8.7-3. The analysis of equation (8.44) can be continued by using an approximation yielding an analytic solution.
As in Chapter 9, we let $n \to \infty$ in the nonlinear Hill function (8.43), so the nonlinearity becomes progressively closer to a step function nonlinearity. Equation (8.44) then becomes

$$\frac{dE(t)}{dt} = -\gamma E(t) + \begin{cases} F_0, & 0 \le E_\tau < \theta, \\ 0, & \theta \le E_\tau. \end{cases} \tag{8.52}$$

The nonlinear differential delay equation (8.52) can be alternatively viewed as a pair of ordinary differential delay equations, and which one we have to solve at any given time depends on the value of the retarded variable E_τ with respect to the parameter θ. (This method of solution is usually called the *method of steps*.)
As initial function for equation (8.52) of the type in (8.45), pick one that satisfies $\phi(t') > \theta$ for $-\tau \le t' \le 0$ and specify that $\phi(0) \equiv E_0$, a constant.

(a) Solve the equation

$$\frac{dE}{dt} = -\gamma E \qquad \theta < E_\tau, \quad E(t=0) \equiv E_0, \tag{8.53}$$

to obtain

$$E(t) = E_0 e^{-\gamma t}, \tag{8.54}$$

valid until a time t_1 determined by the condition $\theta = E(t_1 - \tau)$. Show that the value of t_1 is given by

$$t_1 = \frac{1}{\gamma} \ln \left\{ \frac{E_0 e^{\gamma \tau}}{\theta} \right\}. \tag{8.55}$$

From this value of t_1, show that the value of E at $t = t_1$ can be calculated as

$$E(t = t_1) \equiv E_1 = \theta e^{-\gamma \tau}. \tag{8.56}$$

(b) To proceed for times greater that t_1, solve the other differential equation given in (8.52), namely,

$$\frac{dE}{dt} = -\gamma E + F_0 \qquad E_\tau \le \theta, \quad E(t_1) = E_1, \tag{8.57}$$

to get

$$E(t) = E_1 e^{-\gamma(t-t_1)} + \frac{F_0}{\gamma} \left[1 - e^{-\gamma(t-t_1)} \right], \tag{8.58}$$

which is a solution valid until a time t_2 defined by $\theta = E(t_2 - \tau)$. Compute the value of t_2 as

$$t_2 = \frac{1}{\gamma} \ln \left\{ \left(\frac{E_0}{\theta} \right) \left[\frac{E_1 - (F_0/\gamma)}{\theta - (F_0/\gamma)} \right] e^{2\gamma\tau} \right\}, \tag{8.59}$$

and the value of the solution at time t_2, $(E(t = t_2) \equiv E_2)$ to obtain

$$E_2 = \frac{F_0}{\gamma} + \left(\theta - \frac{F_0}{\gamma} \right) e^{-\gamma\tau}. \tag{8.60}$$

(c) In the computation of the third portion of the solution, you must once again solve equation (8.53) subject to the endpoint conditions determined in the last calculation. Show that

$$E(t) = E_2 e^{-\gamma(t-t_2)} \tag{8.61}$$

is the expression to use, and determine that

$$t_3 = \frac{1}{\gamma} \ln \left\{ \left(\frac{E_0 E_2}{\theta^2} \right) \left[\frac{E_1 - (F_0/\gamma)}{\theta - (F_0/\gamma)} \right] e^{3\gamma\tau} \right\}, \tag{8.62}$$

so that $E(t_3) \equiv E_3$ is given by

$$E_3 = \theta e^{-\gamma\tau}. \tag{8.63}$$

What can you conclude by comparing equations (8.56) and (8.63)? Calculate the period of the periodic solution just derived and show that it is given by

$$T = 2\tau + \frac{1}{\gamma} \ln \left\{ \left[\frac{\frac{F_0}{\gamma\theta}}{\frac{F_0}{\gamma\theta} - 1} - e^{-\gamma\tau} \right] \left[\frac{F_0}{\gamma\theta} - e^{-\gamma\tau} \right] \right\}. \tag{8.64}$$

Ex. 8.7-4. From the previous exercises it seems that first-order differential delay equations with negative feedback have only one bifurcation between a stable steady state and a stable limit cycle when looked at numerically.

However, the situation is quite different if one looks at a system with a *mixed* feedback replacing the negative feedback. Mixed feedback is a term that has been coined to indicate that the feedback function has the characteristics of positive feedback over some range of the state variable, and negative feedback for other ranges.

These systems have a host of bifurcations, and you can explore these numerically by using `XPP` to study the prototype equation

$$\frac{dx}{dt} = -\gamma x + \beta \frac{x_\tau}{1 + x_\tau^n}, \tag{8.65}$$

a variant of which was originally proposed as a model for the regulation of white blood cell production (Mackey and Glass 1977).

(a) How many steady states does equation (8.65) have?
(b) Compute analytically when the steady state becomes unstable in equation (8.65). What is the Hopf period at that point?
(c) Explore the range of behavior that the numerical solutions can take as one changes various parameters. (Note that you can eliminate one of the parameters by, for example, scaling the time by γ so there is only the three–parameter set (β, τ, n) to deal with.)